Available online at www.sciencedirect.com
ScienceDirect
Microelectronic Engineering 84 (2007) 646–652
MICROELECTRONIC ENGINEERING
www.elsevier.com/locate/mee

Effects of plasma treatment on the high frequency characteristics of Cu/Ta/hydrogen silsesquioxane (HSQ) system and electrical behaviors of Cu/Ta/HSQ/Pt MIM capacitors

Chia-Cheng Ho [a], Bi-Shiou Chiou [a,b,*]

[a] *Department of Electronics Engineering and Institute of Electronics, National Chiao Tung University, 1001 Ta Hsueh Road, Hsinchu, Taiwan*
[b] *Innovative Packaging Research Center, National Chiao Tung University, Hsinchu, Taiwan*

Received 29 March 2006; received in revised form 29 September 2006; accepted 25 December 2006
Available online 14 January 2007

Abstract

With the increasing of the operating frequencies, insertion loss, signal propagation delay, and parasitic coupling capacitance become the significant problems. Small capacitance (C) between interconnects is required to reduce the crosstalk, insertion loss, and RC delay associated with the metal interconnect system. Therefore, the interconnect with low dielectric constant (k) material is required. Implementation of Cu/low-k dielectric is used for reducing insertion loss, RC delay, crosstalk noises, etc. In this work, Cu–hydrogen silsesquioxane (HSQ) systems are studied. Ammonia (NH_3) plasma is employed for the nitridation of HSQ. The effects of NH_3 plasma treatments on the high frequency characteristics (100 MHz to 20 GHz) of the interconnect structure Cu/Ta/HSQ and electrical behaviors of Cu/Ta/HSQ/Pt MIM capacitors are evaluated.

Auger electron spectroscopy (AES) results suggest the diffusion of oxygen and copper atoms during copper annealing. This raises resistance of Cu interconnect and increases the conductance of the HSQ films. Hence, 400 °C-annealed Cu/Ta/HSQ interconnect systems become lossy at high frequencies (>2 GHz). Ammonia (NH_3) plasma bombardments break some of the Si–H bonds and the resulting dangling Si bonds increase the moisture absorption. Meanwhile, NH_3 plasma treatments reduce the leakage current by passivating the Si dangling bond and forming silicon nitride. The absorption of moisture and/or the formation of SiN_x result in high dielectric constant of HSQ after prolonged NH_3 plasma bombardment. The dielectric constant of HSQ decreases and then increases with the increase of NH_3 plasma treatment time and a minimum dielectric constant of 2.2 is obtained after 50 s NH_3 plasma treatment at 200 W. Among various specimens in this study, the smallest insertion loss is 1.97 dB/mm at 20 GHz for the 400°C-annealed Cu/Ta/HSQ (NH_3-plasma-treated for 50 s). Appropriate NH_3-plasma bombardment helps to form a thin SiN_x barrier layer which prevents the diffusion of oxygen without increasing the dielectric constant of the Cu–HSQ interconnect system. The leakage currents versus electric field characteristics suggest that a Schottky emission dominate conduction mechanism.

Keywords: Hydrogen silsesquioxane; Interconnect; Insertion loss; Plasma treatment

1. Introduction

As interconnect feature size decreases and clock frequency increases, interconnect RC time delay and insertion loss increment become the major limitation on achieving high circuit speeds and reliability. When operational frequencies are above 1 GHz, the insertion loss resulted from the parasitic effects with the interconnect becomes a limiting factor for chip performance and cannot be ignored [1–3]. In order to retain signal integrity at high frequencies, the interconnect with low dielectric constant (k) dielectric and low resistivity (ρ) conductor was required. Implementation of Cu/low-k dielectrics is used for reducing insertion loss, RC time delay, crosstalk noises, etc. The requirements

---

[*] Corresponding author. Address: Department of Electronics Engineering and Institute of Electronics, National Chiao Tung University, 1001 Ta Hsueh Road, Hsinchu, Taiwan. Tel.: +886 3 5731927; fax: +886 3 5724361.
E-mail address: bschiou@mail.nctu.edu.tw (B.-S. Chiou).

0167-9317/$ - see front matter © 2007 Elsevier B.V. All rights reserved.
doi:10.1016/j.mee.2006.12.010

for the intermetal dielectric includes: a small dielectric constant, a low leakage current, low moisture absorption, adequate mechanical strength, simplicity of process, and ease of integration [4–12].

Hydrogen silsesquioxane (HSQ) is a potential candidate of which the dielectric constant can be further reduced by forming a highly porous three-dimensional network structure [12]. The general formula for HSQ is $(HSiO_{1.5})_{2n}$, $n = 2$, 3, etc., which is an inorganic material that can be considered as a derivative of SiO_2 in which one of the four oxygen atoms bonded to every silicon atom is replaced by hydrogen. However, HSQ has many integration issues, such as thermal dissociation of Si–H bonds, oxidation, plasma damage, formation of –OH bonds, absorption of water, the diffusion of copper into the HSQ films, and/or oxidation of the copper metallization during the thermal treatment [6–8]. Hence, a diffusion barrier is needed to prevent the interdiffusion of Cu and the dielectric layer. However, barrier layer materials usually have a high resistivity or high dielectric constant which increases the RC time delay. Liu et al. reported that nitride barrier layer formed by NH_3 bombardment could prevent the diffusion of Cu into HSQ and maintain low *k* properties of HSQ films [6]. However, the effects of NH_3 plasma treatment on the high frequency electrical properties of HSQ films have not been studied extensively.

In this work, NH_3 plasma is employed for the nitridation of HSQ and the effects of NH_3 plasma treatment on the electrical properties of the interconnect structure Cu/Ta/HSQ are studied. The presence of a Ta barrier not only improves the adhesion between Cu and HSQ but also enhances the Cu microstructure and improves the Cu electromigration resistance [10,11]. The high frequency characteristics of the Cu/Ta/HSQ systems are studied. Besides, the leakage current and dielectric properties of NH_3 plasma-treated HSQ films are investigated.

2. Experimental procedures

Four-inch diameter p-type (1 0 0) Si wafers with nominal resistivity of 10 Ω-cm were used as substrates. The Si wafers were cleaned with the standard RCA cleaning process. Hydrogen silsesquioxane (HSQ) was prepared by spin-coating Dow–Corning Flowable Oxide (FOX) on the wafer and then baked at 150 °C, 250 °C, and 350 °C for 1 min. The curing condition for HSQ films is 400 °C for 1 h in N_2. The thickness of HSQ is about 500 nm after the curing process. Some samples were then subjected to NH_3 plasma treatment for different durations. The NH_3 plasma was operated at a pressure of 300 mtorr and with a NH_3 gas flow rate of 500 sccm in a plasma-enhanced chemical vapor deposition reaction chamber. An rf power of 200 W, which established the NH_3 plasma, was applied to the HSQ films at a substrate temperature of 300 °C and a chamber temperature of 250 °C. The tantalum (50 nm) and copper (450 nm) films were sputtered sequentially and then annealed at 400 °C for 1 h in N_2 at a pressure of 10 torr. Low pressure annealing avoids the oxidation of copper films. For dielectric property measurements, metal–insulator–metal (MIM) capacitors with Cu/Ta/HSQ/Pt/Ta/SiO_2/Si multilayer structure were prepared. For *S*-parameter measurements, a Cu/Ta/HSQ/SiO_2/Si multilayer structure was used and conventional lithographic processes were employed to obtain the interconnect patterns.

A C–V analyzer (model 590, Keithley Instruments Inc., USA) and a semiconductor parameter analyzer (HP4155B, Hewlett–Packard Co., USA) were employed to measure the capacitance and the leakage current of the MIM capacitors, respectively. A Cascade Microtech Probe Station and a Network Analyzer (HP-85122A, Hewlett–Packard Co., USA) which operates from 100 MHz to 20 GHz were used to measure the *S*-parameters of the interconnect on-wafer with the microwave probes. Before each measurement, calibrations were carried out with SOLT pads (short, open, load, and through) purchased from Cascade Microtech (Cascade Microtech, USA). A de-embedding method [14] was employed to subtract the shunt parasitics of the probing pads. Composition depth profile analysis was performed with Auger electron spectrometry (670 PHI Xi, Physical Electronics, USA). The chemical bonds of HSQ films were investigated by Fourier transform infrared reflection absorption spectrometer (FTIR-RAS). The FTIR-RAS system used in this study (DA8.3, Bomen Inc., Canada) was a stand-alone measurement system. Its beam was P-polarized incident beam and scan mode was 75° grazing incident angle reflectance because the samples were thin films. Two hundred scans were carried out and the resolution was $\sim 1\ cm^{-1}$.

3. Results and discussion

The typical structure of HSQ, as shown in Fig. 1a, is an Si–O cage containing Si–H bonds and the three-dimensional (3D) network structure can be obtained after the curing process. Fig. 1b shows the FTIR-RAS spectra of specimens as a function of NH_3 plasma treatment time. The bond wavenumbers of various absorption peaks are summarized in Fig. 1a [8,15]. Fig. 1c gives the peak ratio of the bonds with respect to the bonds of the as-cured HSQ films. Plasma treatment breaks the Si–H, Si–O bending cage-like, and Si–O bending network bonds. The Si–O bending cage-like peak ratio ($895\ cm^{-1}$), the Si–O bending network peak ratio ($822\ cm^{-1}$), and the Si–H peak ratio ($2250\ cm^{-1}$) decrease with the increase of NH_3 plasma bombardment time, while the Si–N peak ratio ($985\ cm^{-1}$) increases with plasma bombardment time. Also shown in Fig. 1c is the peak ratio of specimens subjected to 1800 s O_2 plasma treatment. The peak ratios of HSQ films subjected to O_2 plasma treatment are lower than those subjected to NH_3 plasma treatment.

Fig. 2 gives the dielectric constant and dissipation factor of MIM capacitors as a function of plasma treatment duration. The dielectric constant decreases initially and

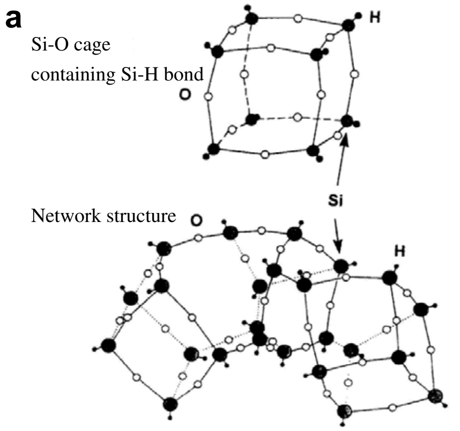

IR Absorption location (cm^{-1})	Assignment
2250	Si-H
1150	Si-O stretching cage-like
1060	Si-O stretching network
985	Si-N
895	Si-O bending cage-like
822	Si-O bending network

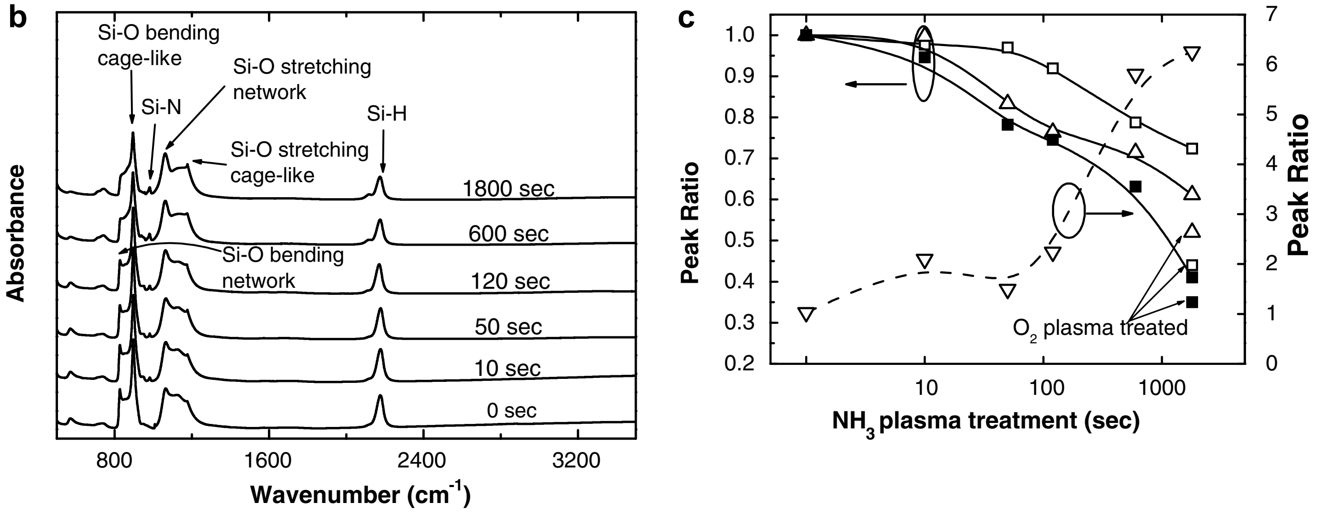

Fig. 1. (a) Schematic diagram of the structure of hydrogen silsesquioxane (HSQ) and infrared absorption assignments applicable to HSQ films [13,15], (b) FTIR spectra of HSQ versus NH$_3$ plasma treatment time, and (c) absorbance peak ratio of bond with respect to that of the as-cured HSQ films as a function of NH$_3$ plasma treatment time. The absorbance wavenumbers are 985 cm^{-1} for Si–N peak (▽), 2250 cm^{-1} for Si–H peak (△), 895 cm^{-1} for Si–O bending cage-like peak (□), and 822 cm^{-1} for Si–O bending network peak (■). Also shown in Fig. 1c are the peak ratios of specimens treated with O$_2$ plasma for 1800 s.

then increases with the increase of NH$_3$ plasma treatment time. For HSQ films, each silicon atom is bonded to three oxygen atoms and one hydrogen atom. However, some Si–H bonds Ibreak during curing and/or plasma bombardment and the resulting dangling Si bonds increase the moisture absorption [8,13,16]. As indicated in Fig. 1c, Si–H bond intensity decreases and Si–N bond intensity increases after NH$_3$ plasma treatment. It is argued that NH$_3$ plasma bombardment not only breaks the Si–H bonds but also supplies N atoms to form the SiN$_x$ films. The former creates dangling Si bonds which result in moisture absorption and consequently an increase in dielectric constant, while the latter passivates the dangling Si bonds and forms the SiN$_x$ films. The increase of the dielectric constant after prolonged NH$_3$ plasma bombardment is attributed to the absorption of the moisture and/or the formation of high dielectric constant SiN$_x$ films (~7.9). A minimum dielectric constant of ~2.2 and a minimum dissipation factor of 8.5×10^{-3} are obtained after 50 s NH$_3$ plasma bombardment. HSQ films bombarded by O$_2$ plasma have a dielectric constant of ~ 3.4 and a dissipation factor of $\sim 2 \times 10^{-2}$ which are smaller than those of HSQ films subjected to NH$_3$ plasma treatment for the same period of time.

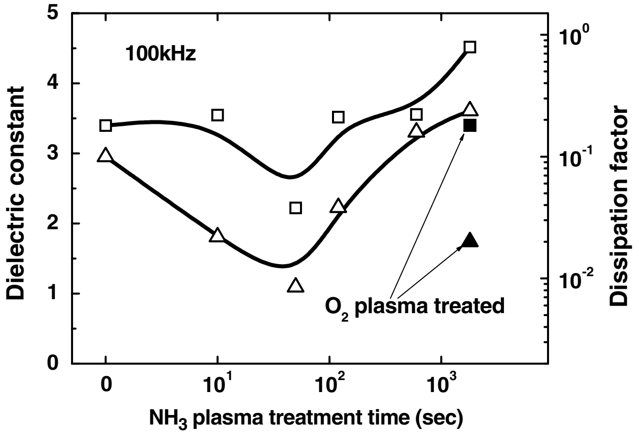

Fig. 2. Dielectric constant (□) and dissipation factor (ρ) of HSQ as a function of NH$_3$ plasma treatment time. Data of HSQ treated with O$_2$ plasma for 1800 s are also shown (■, ▲) for comparison.

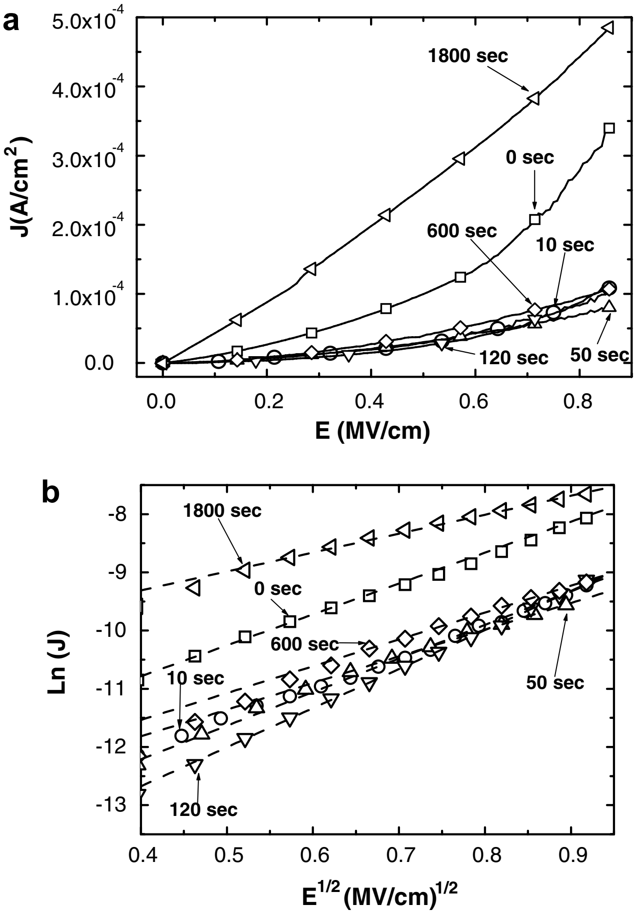

Fig. 3. (a) Leakage current density (J) versus electric field (E) and (b) Ln(J) versus $E^{1/2}$ of Cu/Ta/HSQ/Pt MIM capacitors of which HSQ dielectric subjected to NH_3 plasma treatment for various durations. Data measured at 425 K.

Fig. 3 exhibits the leakage current density (J) versus electric field (E) characteristics of the MIM capacitors as a function of plasma treatment time. A linear relationship is obtained on the Ln(J) versus $E^{1/2}$, as shown in Fig. 3b, which suggests Schottky emission (SE) or Poole–Frenkel (PF) emission mechanisms [6,17]. The leakage current densities of the two conduction mechanisms are expressed as follows:*for SE emission*:

$$\mathrm{Ln}\left(\frac{J_{\mathrm{SE}}}{A*T^2}\right) = \frac{\beta_{\mathrm{SE}}\sqrt{E} - \phi_{\mathrm{SE}}}{k_{\mathrm{B}}T} \tag{1}$$

for PF emission:

$$\mathrm{Ln}\left(\frac{J_{\mathrm{PF}}}{J_0}\right) = \frac{\beta_{\mathrm{PF}}\sqrt{E} - \phi_{\mathrm{PF}}}{k_{\mathrm{B}}T} \tag{2}$$

where $\beta_{\mathrm{SE}} = (e^3/4\,\pi\varepsilon_0\varepsilon_\infty)^{1/2}$, A^* is the effective Richardson's constant (120 A/cm^2/K^2), ϕ_{SE} is the potential barrier height at the surface, ε_0 is the dynamic dielectric constant of free space, ε_∞ is the high frequency dielectric constant, e is the unit charge, k_{B} is Boltzmann's constant, T is absolute temperature, E is external electric field, $\beta_{\mathrm{PF}} = (e^3/\pi\varepsilon_0\varepsilon_\infty)^{1/2}$, and ϕ_{PF} is the potential barrier height of trap potential well. The PF transport mechanism is a result of the lowering of the barrier height of traps in the dielectrics.

The slope of the Ln(J) versus $E^{1/2}$ curve, as summarized in Table 1, is β/kT where β is β_{SE} (for Schottky emission) or β_{PF} (for Poole–Frenkel emission). Both β_{SE} and β_{PF} are calculated and listed in Table 1 for comparison. The β values obtained in this study are closer to β_{SE} and this suggests that the dominant mechanism for charge carriers to transport in HSQ is Schottky emission. The potential barrier heights (ϕ_{SE}) of the Schottky emission model are thus calculated and listed on Table 1. The barrier height increases from 1.27 eV of the as-cured HSQ to a maximum of 1.39 eV of the 120 s plasma-treated HSQ and then decreases to 1.18 eV of the 1800 s plasma-treated HSQ. As mentioned previously, the FTIR-RAS spectra indicate a decrease of the Si–H bonds after plasma treatment. In addition to, an increase in Si–N bonds, which suggests nitridation reactions to repassivation of dangling Si bonds and formation of SiN_x films, is observed after NH_3 plasma treatment for longer than 50 s. It is not clear at this moment why the barrier height and the dielectric constant decrease with the increase of plasma bombardment for HSQ films subjected to short duration of NH_3 plasma treatment (i.e., $\leqslant$50 s). There are many factors that affect

Table 1
The slope ($\beta/k_{\mathrm{B}}T$)of the Ln(J) versus $E^{1/2}$ plots shown in Fig. 3b and the parameters extracted from curve fitting of the Schottky emission model and Poole–Frenkel emission model[a]

NH_3 plasma treatment time (s)	Slope ($\beta/k_{\mathrm{B}}T$) (m/V)$^{1/2}$	β (10^{-24} J m$^{1/2}$/V$^{1/2}$)	β_{SE} (10^{-24} J m$^{1/2}$/V$^{1/2}$)	β_{PF} (10^{-24} J m$^{1/2}$/V$^{1/2}$)	ϕ_{SE} (eV)
0	5.31	3.1	4.4	8.7	1.27
10	4.58	2.7	4.3	8.7	1.30
50	5.77	3.4	4.5	9.0	1.33
120	6.71	3.9	4.3	8.7	1.39
600	4.61	2.7	4.3	8.7	1.29
1800	3.25	1.9	4.3	8.5	1.18

[a] SE emission model : $\mathrm{Ln}\left(\frac{J_{\mathrm{SE}}}{A*T^2}\right) = \frac{\beta_{\mathrm{SE}}\sqrt{E}-\phi_{\mathrm{SE}}}{k_{\mathrm{B}}T}$.

PF emission model : $Ln\left(\frac{J_{\mathrm{PF}}}{J_0}\right) = \frac{\beta_{\mathrm{PF}}\sqrt{E}-\phi_{\mathrm{PF}}}{k_{\mathrm{B}}T}$.

where a ϕ_{SE} is the potential barrier height at the surface, a ϕ_{PF} is the trap energy level, k_{B} is Boltzmann's constant, and T is the temperature of measurement (425 K).

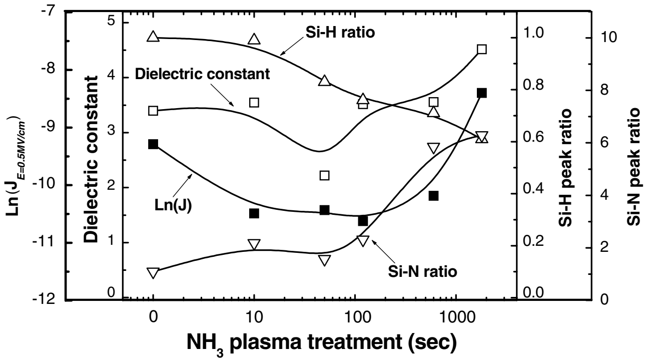

Fig. 4. Leakage current density (J) at 0.5 MV/cm (■), dielectric constant (□) at 100 kHz, Si–H peak ratio (△), and Si–N peak ratio (▽) of HSQ films as a function of NH_3 plasma treatment time.

the barrier height, such as the work function of the electrode metal, electron affinity of the dielectric, and the surface states. Nevertheless, the decrease of the barrier height as well as the increase of both the leakage current and the dielectric constant after HSQ subjected to prolonged plasma treatment are attributed to the moisture absorption and the formation of SiN_x which has a higher dielectric constant (7.8). Fig. 4 exhibits the leakage current, the dielectric constant, the Si–N peak ratio, and the Si–H peak ratio as functions of NH_3 plasma treatment time.

The test structure for insertion loss measurement has one signal line as exhibited in Fig. 5a. With the ground–signal–ground probes, insertion loss (dB/mm) is obtained from the S-parameters S_{21} and S_{11}.

$$\text{Insertion loss} = 10 \times \text{Log}\left(\frac{|S_{21}|^2}{1-|S_{11}|^2}\right) \times \frac{1}{\text{length}}\,(\text{dB/mm}) \tag{3}$$

Fig. 5b exhibits the insertion loss and the S_{21} parameter of the as-deposited Cu/Ta interconnect on HSQ (□) and the 400 °C-annealed Cu/Ta interconnect on HSQ (△), the 400 °C-annealed Cu/Ta interconnect on HSQ treated with NH_3 plasma for 50 s (○), and the 400 °C-annealed Cu/Ta interconnect on HSQ treated with NH_3 plasma for 1800 s (•). Annealing raises the insertion loss (i.e., decreases S_{21}) of the interconnect. The as-deposited Cu/Ta/HSQ interconnect has the smaller insertion loss, i.e., the larger S_{21}, than the 400 °C-annealed Cu/Ta/HSQ, as shown in Fig. 5b. Plasma treatment for a short duration decreases the insertion loss of the interconnect. Specimens subjected to 50 s NH_3 plasma bombardment show the smallest insertion loss (the largest S_{21}) among all specimens in this study. However, prolonged NH_3 plasma bombardment increases the insertion loss. The insertion losses are 2.44 dB/mm, 2.45 dB/mm, 1.66 dB/mm, and 3.67 dB/mm at 10 GHz, and 2.60 dB/mm, 2.63 dB/mm, 1.97 dB/mm, and 4.09 dB/mm at 20 GHz for the as-deposited Cu/Ta/HSQ, the 400 °C-annealed Cu/Ta/HSQ, the 400°C-annealed Cu/

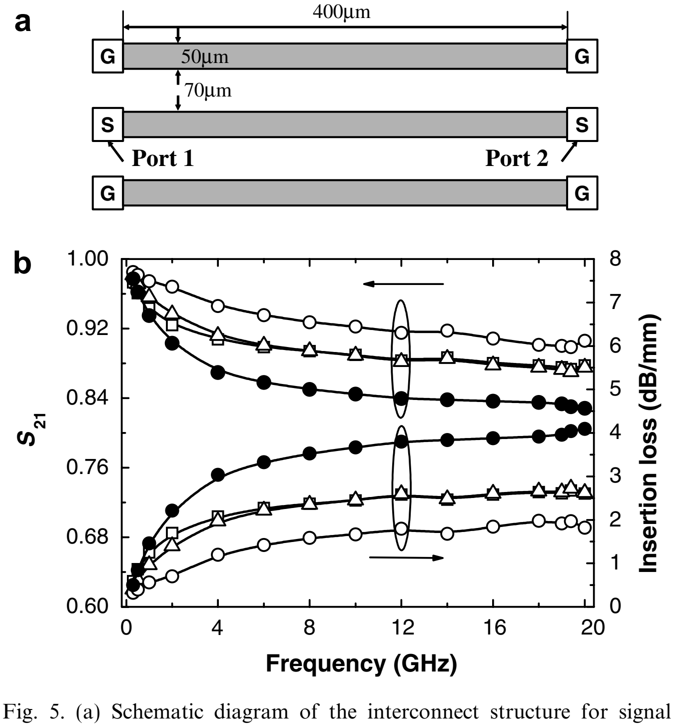

Fig. 5. (a) Schematic diagram of the interconnect structure for signal attenuation measurement, and (b) insertion loss and S-parameter S_{21} as a function of frequency of the as-deposited Cu/Ta/HSQ (□), the 400 °C-annealed Cu/Ta/HSQ (△), the 400 °C-annealed Cu/Ta/HSQ (NH_3-plasma-treated for 50 s) (○), and the 400 °C-annealed Cu/Ta/HSQ(NH_3-plasma-treated for 1800 s) (●).

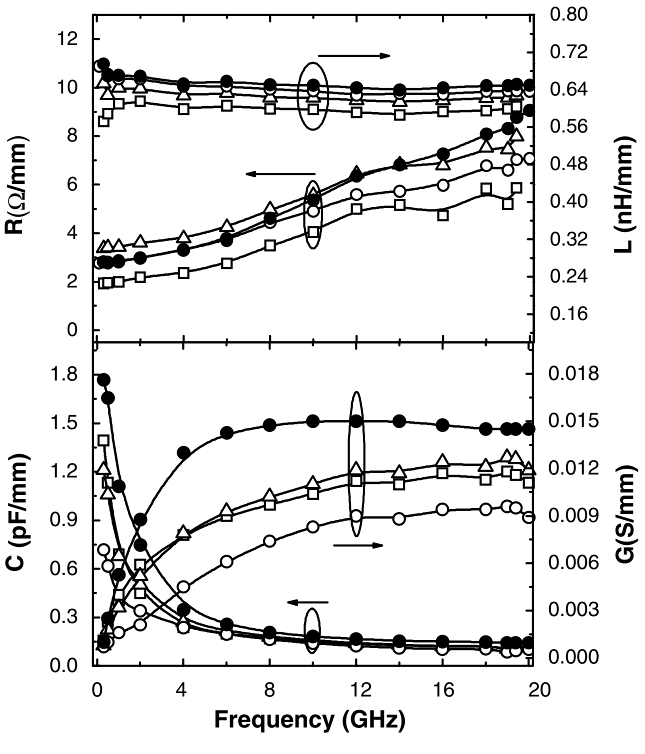

Fig. 6. Inductance (L), resistance (R), capacitance (C), and conductance (G) as a function of frequency of the as-deposited Cu/Ta/HSQ (□), the 400 °C-annealed Cu/Ta/HSQ (△), the 400 °C-annealed Cu/Ta/HSQ(NH_3-plasma-treated for 50 s) (○), and the 400 °C-annealed Cu/Ta/HSQ (NH_3-plasma-treated for 1800 s) (●).

Ta/HSQ (NH_3-plasma-treated for 50 s), and the 400°C-annealed Cu/Ta/HSQ (NH_3-plasma-treated for 1800 s), respectively.

The interconnect transmission parameters *R*, *L*, *C*, and *G*, as shown in Fig. 6, are calculated from the measured *S*-parameters [18]. The *R*, *L*, *C*, and *G* are the resistance, inductance, capacitance, and conductance per unit length of the interconnect, respectively.

The resistance (*R*) of the interconnect increases with the increasing of applied frequency. Skin effect is one of the major reasons which cause the increase of *R* with the frequency. Interconnect with the as-deposited Cu/Ta/HSQ shows the lowest resistance. The interconnect inductance, resulted from magnetic flux enclosed between the signal line and the return path, is dependent on the space to the return path and is relatively constant over frequency. Specimen with the as-deposited Cu/Ta/HSQ has smaller conductance (*G*) than those with the 400 °C-annealed Cu/Ta/HSQ. The conductance (*G*) of the HSQ

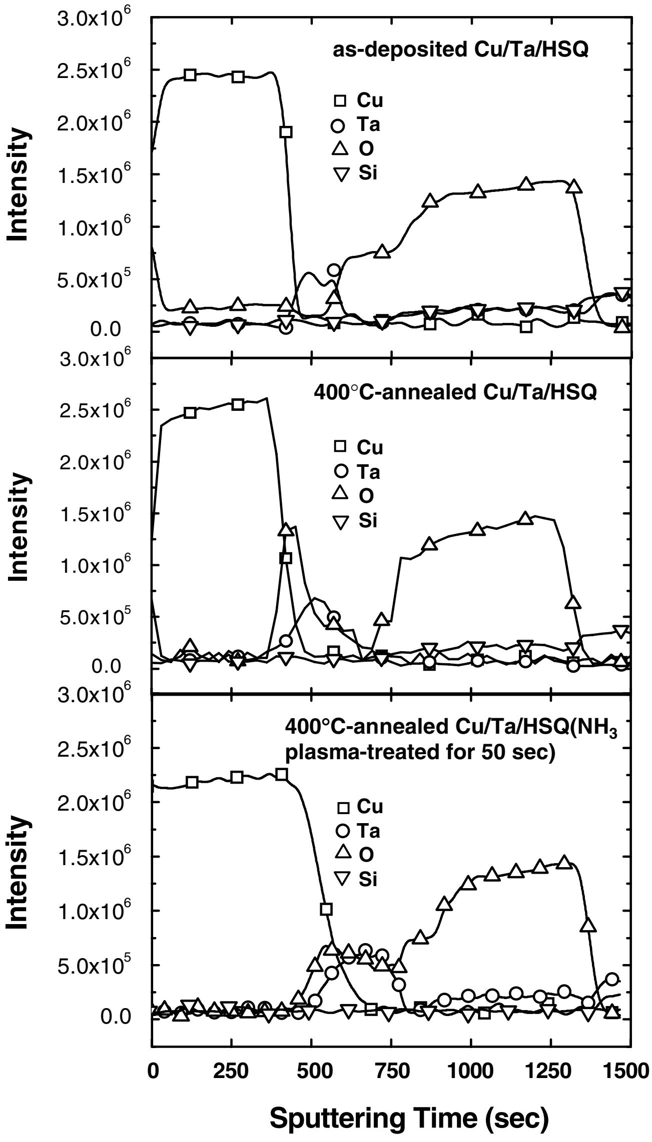

Fig. 7. AES depth profiles of three specimens in this study.

Table 2

S_{21}, insertion loss, inductance (*L*), resistance (*R*), capacitance (*C*), conductance (*G*), dielectric constant (*k*), leakage current density (*J*), Si–H peak ratio, and Si–N peak ratio of various specimens in this work

Specimen	S_{21} [a]	Insertion loss[a] (dB/mm)	R^a (Ω/mm)	L^a (nH/mm)	C^a (pF/mm)	G^a (S/mm)	*k*(100 kHz)	J^b (A/cm^2)	Si–H peak ratio	Si–N peak ratio
As-deposited Cu/Ta/HSQ(0)[c]	0.87	2.60	9.92	0.61	0.12	0.0111	3.40	2.79	1	1
400 °C-annealed Cu/Ta/HSQ(0)[c]	0.88	2.63	7.99	0.63	0.12	0.0119	3.54	1.53	0.99	0.21
400 °C-annealed Cu/Ta/HSQ(50)[c]	0.91	1.82	7.08	0.64	0.10	0.0089	2.31	1.59	0.83	0.149
400 °C-annealed Cu/Ta/HSQ(120)[c]	–	–	–	–	–	–	3.52	1.39	0.76	0.223
400 °C-annealed Cu/Ta/HSQ(600)[c]	–	–	–	–	–	–	3.56	1.85	0.71	0.58
400 °C-annealed Cu/Ta/HSQ(1800)[c]	0.83	4.09	9.06	0.65	0.14	0.0145	4.52	3.72	0.61	0.625

[a] Measured at 20 GHz.

[b] Measured at 0.5 MV/cm.

[c] Datum in the parenthesis ( ) is the NH_3 plasma treatment time in seconds.

treated with NH_3 plasma for 50 s is the smallest among all specimens in this study. However, the prolonged NH_3 plasma treatment (1800 s) degrades HSQ films, and both the conductance (G) and the capacitance (C) of the HSQ dielectric increase. This is consistent with the increase of the insertion loss discussed previously. Also observed in Fig. 6 is an abrupt decrease of the capacitance at 1.2 GHz. It is argued that this is due to change of the interconnect propagation mode from slow-wave mode to Quasi-TEM mode [13].

The 400 °C-annealed Cu/Ta/HSQ has larger R and G as compared to the as-deposited Cu/Ta/HSQ. The Auger electron spectroscopy (AES) results, as shown in Fig. 7, suggest the diffusion of oxygen atoms into Cu films after annealing. The increase in R is attributed to the oxidation of Cu interconnect and the increase of G could be caused by the diffusion of Cu and Ta into HSQ films after annealing. Table 2 summarizes the S_{21}, insertion loss, inductance (L), resistance (R), capacitance (C), conductance (G), dielectric constant (k), leakage current density (J), Si–H peak ratio, and Si–N peak ratio of various specimens in this study.

4. Conclusions

In this study, NH_3 plasma treatment is employed to form silicon nitride on HSQ films to prevent the diffusion of oxygen and oxidation of copper. However, the effect of NH_3 plasma treatment is multiple. Besides forming SiN_x, plasma bombardments break the Si–H bonds and result in hygroscopic Si dangling bonds. The dielectric constant of HSQ decreases and then increases with the increase of NH_3 plasma treatment time and a minimum dielectric constant of 2.2 is obtained after 50 s NH_3 plasma treatment at 200 W.

Among various specimens in this study, the smallest insertion loss is 1.97 dB/mm at 20 GHz for the 400 °C-annealed Cu/Ta/HSQ(NH_3-plasma-treated for 50 s). Appropriate NH_3-plasma bombardment helps to form a thin SiN_x barrier layer which prevents the diffusion of oxygen without increasing the dielectric constant of the Cu–HSQ interconnect system. The leakage currents versus electric field characteristics suggest that a Schottky emission dominate conduction mechanism.

The barrier height for Schottky emission increases from 1.27 eV of the as-cured HSQ to a maximum of 1.39 eV of the 120 s plasma-treated HSQ and then decreases to 1.18 eV of the 1800 s plasma-treated HSQ. The decrease of the barrier height as well as the increase of both the leakage current and the dielectric constant after HSQ subjected to prolonged plasma treatment are attributed to the moisture absorption and the formation of SiN_x.

Acknowledgements

This work is sponsored by National Science Council, Taiwan, under the Contract No. NSC 93-2216-E-009-023.

References

[1] Semiconductor Industry Associations, International Technology Roadmap for Semiconductors, 2004. <http://public.itrs.net/Files/2004UpdateFinal/ 2004Update.htm.>.
[2] P. Heydari, S. Abbaspour, M. Pedram, in: Proceedings of the International Conference on VLSI Design, 2002, pp. 132–137.
[3] S.S. Wong, P. Yue, R. Chang, S.Y. Kim, B. Kleveland, F. O'Mahony, in: Proceedings of the International Symposium on Quality Electronic Design, 2003, pp. 1–6.
[4] Z. Chen, K. Prasad, C. Li, N. Jiang, D. Gui, IEEE Trans. Dev. Mater. Reliab. 5 (2005) 133–141.
[5] K. Char, B.J. Cha, S. Kim, in: Proceedings of the International Interconnect Technology Conference, 2004, pp. 219–221.
[6] P.T. Liu, T.C. Chang, Y.L. Yang, S.M. Sze, IEEE Trans. Electron Dev. 47 (2000) 1733–1739.
[7] P.T. Liu, T.C. Chang, S.M. Sze, F.M. Pan, Y.J. Mei, W.F. Wu, M.S. Tsai, B.T. Dai, C.Y. Chang, F.Y. Shih, H.D. Huang, Thin Solid Films 332 (1998) 345–350.
[8] C.T. Chen, B.S. Chiou, J. Mater. Sci. Mater. Electron. 15 (2004) 139–143.
[9] H.S. Tzeng, B.S. Chiou, W.F. Wu, C.C. Ho, J. Electron. Mater. 33 (2004) 796–801.
[10] C.T. Chen, B.S. Chiou, J. Electron. Mater. 33 (2004) 368–373.
[11] W.L. Sung, B.S. Chiou, J. Electron. Mater. 31 (2002) 472–477.
[12] S.P. Jeng, K. Taylor, T. Seha, M.C. Chang, J. Fattaruso, R.H. Havemann, in: Proceedings of the Symposium on VLSI Technology Digest of Technical Papers, 1995, pp. 61–62.
[13] C.C. Ho, B.S. Chiou, Microelectr. Eng. 83 (2006) 528–535.
[14] H. Cho, D.E. Burk, IEEE Trans. Electron Dev. 38 (1991) 1371–1375.
[15] M.J. Loboda, C.M. Grove, R.F. Schneider, J. Electrochem. Soc. 145 (1998) 2861–2866.
[16] P.T. Liu, T.C. Chang, Y.L. Yang, Y.F. Chen, J.K. Lee, F.Y. Shih, E. Tsai, G. Chen, S.M. Sze, J. Electrochem. Soc. 147 (2000) 1186–1192.
[17] S.M. Sze, Physics of Semiconductor Devices, second ed., Wiley, New York, 1981.
[18] David M. Pozar, Microwave Engineering, second ed., Wiley, New York, 1998.